Designing a Condense-Air Separator for a Double-Stage Oil Injected Screw Compressor and Verification by Two-Phase Discrete Phase Modelling CFD Analysis

Sinan PİŞİRİCİ

Hükümran Selim Ertürk

Buğrahan Bahadır

Designing a Condense-Air Separator for a Double-Stage Oil Injected Screw Compressor and Verification by Two-Phase Discrete Phase Modelling CFD Analysis

Buğrahan BAHADIR[1]*, Hükümran Selim ERTÜRK[1], Sinan PİŞİRİCİ[1]

[1]Dalgakıran Compressor, Research & Development,
Istanbul, Turkey
bugra.bahadir@dalgakiran.com, selim.erturk@dalgakiran.com, sinan.pisirici@dalgakiran.com

* Corresponding Author

ABSTRACT

Air-Condense separators used at the outlet of oil-injected screw compressors play a very key role. As much as possible, zero amount of water should reach to the air dryer at the compressor outlet. The air dryers used at the compressor outlet are for absorbing the moisture in the air. If the excess condensate goes to the dryer, it will cause it to not work at the desired performance and this will cause corrosion in the user's compressed air line and damage the equipment where compressed air is used. For this reason, while maximizing the separation efficiency is important, a design study is made in which pressure drops are optimized and compressor energy consumption is reduced. Some of the most efficient and cost-effective separators use the cyclone separation method. This method has been selected for the new separator designs. First a mathematical method has been devised based on the literature on cyclones and swirl tubes. This method has been used to calculate outputs and design swirl tube air-condense separator model. The designs were verified for separation efficiency and pressure drops by using "Discrete Phase Modelling" two-phase fluid flow simulations and analyses. The verified designs were manufactured as prototypes and installed to a test compressor. In order to determine the most optimal among the new designs made, tests were carried out and the necessary results were compared. At the end, the aim of manufacturing new air-condense separators with a higher separation efficiency than the older ones were achieved.

1. INTRODUCTION

A family of double-stage Oil Injected Screw Compressors with powers ranging from 90-110 kW produced and designed by Dalgakıran Compressor have been selected for condense separation design update. In this project, redesigning of condense separators after the air cooler is included. Previously, condense separators that are used after the air cooler are supplied from the Dalgakıran's supplier. In this study, Dalgakıran Compressor designed and produced their own condense separators. The reason why this need was arose was due to the fact that the dimensions of the suppliers products were to large to integrate the separators in the compressor cabin. While this design was designed in a small way in accordance with the machine construction, pressure losses and separation efficiencies were also optimized. With the rapidly increasing awareness of energy efficiency in the world, pressure loss optimization was an important parameter as well as separation efficiency, as it is a component that also makes a significant contribution to machine internal pressure losses.

Compressor has one condense separator after the air cooler. After the compressed air enters the cooler, it is cooled to approximately 10 degrees above the ambient. A condense separator is needed at the outlet of the cooler to separate the condensed water. This condense is not wanted in the compressed air usage areas.

With the design, CFD and test knowledge it has made regarding the water separator in the compressor sector, Dalgakıran has reached a knowledge that can easily find special solutions for its own products from now on. Instead of the large and costly water separators currently used, a pressure drop-optimized design with the same efficiency has been developed, and it has started to produce energy efficiency and high-quality compressed air solutions for customers.

2. MATHEMATICAL MODEL

Sizing of the swirl tube designs were made by using a slightly modified Muschelknautz model. Since the efficiency of the liquid-gas separators depend mainly on the particle distribution entering from the inlet, this distribution was investigated at first.

The operating conditions of the compressor have been used to calculate the volumetric and mass flow rates for both the air and total water phases inside the system. The conditions after the heat exchangers have been used to calculate how much of the vaporous phase of water would be condensed into liquid water. For most of the calculations in the design, the operating conditions have been taken as 20 °C ambient temperature 1 bara ambient pressure and %80 humidity.

In the design below, there are 2 concentric pipes, the one in the outer side is larger than the inner one. Below, the cross sectional are between the two of them is to drain the water from the system. While designing, attention was paid to be compact, as small as possible, and in a structure that would provide maximum efficiency.

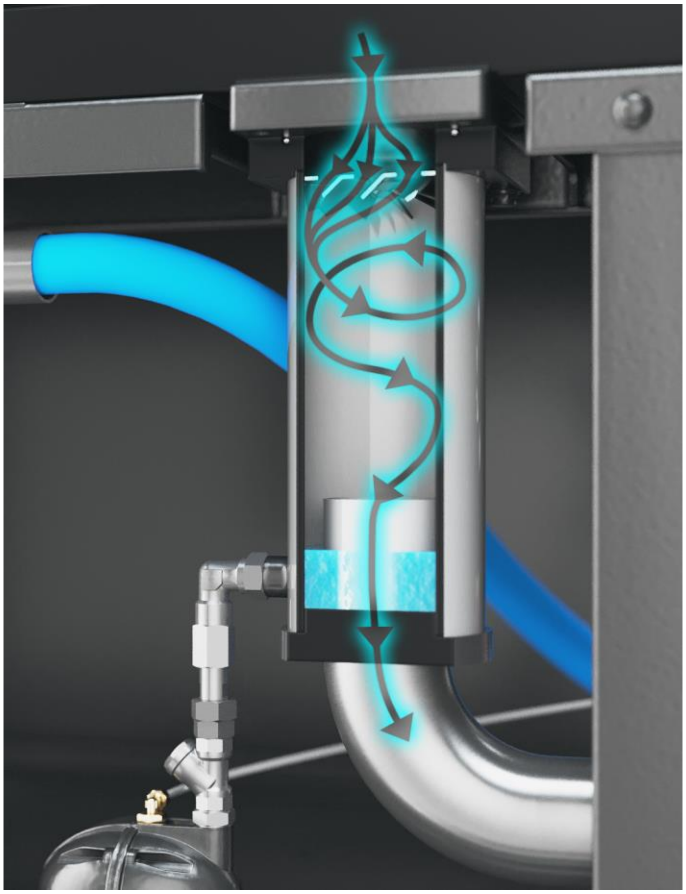

Figure 1: Water (Condense) Separator

In this mathematical model, our crucial design parameters are swirl vane inner boss diameter, swirl vane angle, vane internal diameter, number of vane elements, vane thickness and vane external diameter. In order to find the Throat Area the formula below is used for orthogonal vanes.

$$A_{th} = \frac{1}{2}(\pi D_{iv} sin\beta - N_v t)(D_{ov} - D_{iv}) \quad (1)$$

Depending on the throat area, throat velocity can be calculated. Then Tangential velocity can be calculated as well.

$$Q = V_{(th)} * A_{(th)} \quad (2)$$

$$V_0 = V_{th} cos\beta \quad (3)$$

In this model, "Harwell" technique is used in order to calculate an estimate particle size. The particle sizes that are expected may be smaller than what would happen in real life because the concentration dependent term is neglected. The formula below, 'sauter mean' calculates the diameter sizes of the droplets. (Hoffmann and Stein, 2010).

$$X_{Sa} = 1.91 D_t \frac{Re^{0.1}}{We^{0.6}} (\frac{\rho}{\rho_t})^{0.6} \quad (4)$$

Inlet pipe Reynolds number and inlet pipe weber number formulas are shown below.

$$Re = \frac{\rho V_t D_t}{\mu} \quad We = \frac{\rho V_t^2 D_t}{\sigma} \quad (5)$$

The volume-median droplet diameter can be found by using the Sauter-mean diameter as follows.

$$X_{med} = 1.42 x_{sa} \quad (6)$$

After Sauter-mean diameters are found, minimum, maximum and mean diameters can be calculated. These values were also the inputs of the rosin rammler distribution in the CFD study for the particle diameters.

2. DESIGN STUDY

As the machine dimensions were optimized, we had design limits that were constructively prohibitive inside the water separator.

2.1 Design Geometry and Limitations

In this design, there were some design limits such as diameter and the height of the separator. The diameter needed to be same in order to be compatible with the air coolers outlet and also there is maximum of 550 mm for the height of the separator because the outlet of the air cooler is at the downside. The condense separators we use in the standard are about 1 meter long and are a type that first provides the cyclone movement in the down direction, then continues the separation with the effect of gravity and works by the upward movement of the air. In this design, the cyclone moves downward and then the air exits downward.

2.2 CFD Modelling

2.2.1 Selection of turbulence model

In this study, the turbulence model used for CFD analysis is the RNG k - ε model. The purpose of choosing this model;

- The RNG model has an additional term in its ε equation that significantly improves the accuracy for rapidly strained flows.
- The effect of swirl on turbulence is included in the RNG model, enhancing accuracy for swirling flows.
- The RNG theory provides an analytical formula for turbulent Prandtl numbers, while the standard k - ε model uses user-specified, constant values.

- While the standard k - ε model is a high-Reynolds-number model, the RNG theory provides an analytically-derived differential formula for effective viscosity that accounts for low-Reynolds-number effects. Effective use of this feature does, however, depend on an appropriate treatment of the near-wall region.

These features make the RNG k - ε model more accurate and reliable for a wider class of flows than the standard k - ε model.

2.2.2 Meshing

In this study, Multizone and inflations are used for good mesh quality. Approximately 780.000 nodes are created. And mesh quality is observed 0,24 skewness value in average. Also added inflation layers to improve wall-fluid interactions.

To create more efficient meshes on wing zone, Patch independent mesh method is used in the case. Proximity and Cuvature feature is on. Minimum mesh size is 3 mm. Maximum mesh size is 6 mm. There are samples about meshing in the below.

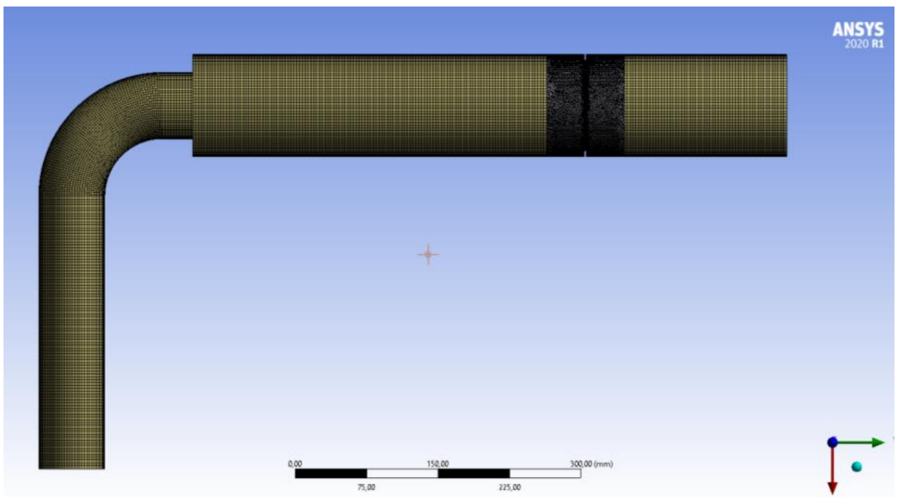

Figure 2: Patch conforming and full body meshing view.

2.2.3 Fluent model

In this study, CFD models sample that in the below is used for every CFD simulations. Apart from the parameters in the table, changes in geometry, air velocity and particle diameters were calculated separately for each CFD analysis. These parameters are commonly used in every CFD project.

Table 1 CFD Parameters

General settings	Pressure-based, Steady, gravity magnitude (-9.81 Y)
Models	RNG k - ε model, Swirl dominated, Standard wall functions, Curvature Correction (on),
Discrete Phase Model	Injection from inlet surface, Diameter distribution is Rosin-Rammler, Material = Water-liquid
Methods	Scheme = Coupled Gradient = Least Squares Cell Based Pressure = Second Order Momentum = Second Order Turbulent kinetic energy = First order upwind Turbulent dissipation rate = First order upwind Pseudo Transient = On

Along the simulation works, particle tracks had been worked also in simulations. Particle trapping, escaping or incompletes were tracked.

After simulation particle tracking histories, diameter of particles, velocities and any other magnitudes that would be needed are exported for the results.

2.2.5 CFD results

After fluent solver exported particle tracking were imported to Results. All simulation results were transformed to observe particle diameters, particle masses, particle swirl velocities and system pressure drops efficiently in results page to compare test results.

There is an example of a visualized particle tracking of diameter of water in the below.

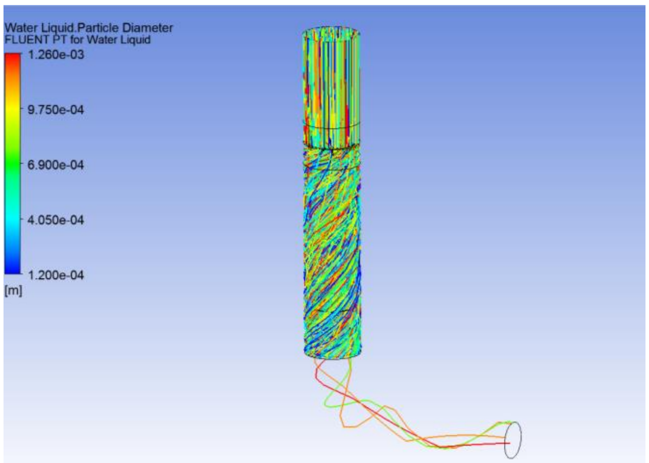

Figure 3: Particle tracking that escaped particles diameter

3. EXPERIMENTAL SETUP

After the design and production process, the separator was produced and mounted right after the compressor's cooler. A pressure transmitter was connected to its inlet and outlet, and differential pressure records were taken from here and saved to datalogger DEWESOFT DEWE-43A. For the pressure transmitters, it was decided to use Keller PAA-M5 HB type pressure transmitters which has ±0,1 % accuracy.

Figure 4: Water (Condense) Separator

There is a mechanical drain at the outlet of the condensate separator. The condensate is discharged from here to a little container that will prevent the condensate from decreasing in case of evaporation, with a zero loss drain. The test was carried out when the ambient pressure was 0.997 bar, the ambient temperature was 20 degrees and the relative humidity was 58%.

4. RESULTS AND DISCUSSION

4.1 CFD Results and Optimization

In this CFD optimization study, the separation efficiency was observed by optimizing the 3 geometric properties of the condense seperator. One of these geometric feature is throat area, one is cyclone length and the other is vane angle. Two different throat areas, two different cyclone lengths and five different vane angles, optimization studies were carried out with a total of 20 CFD studies.

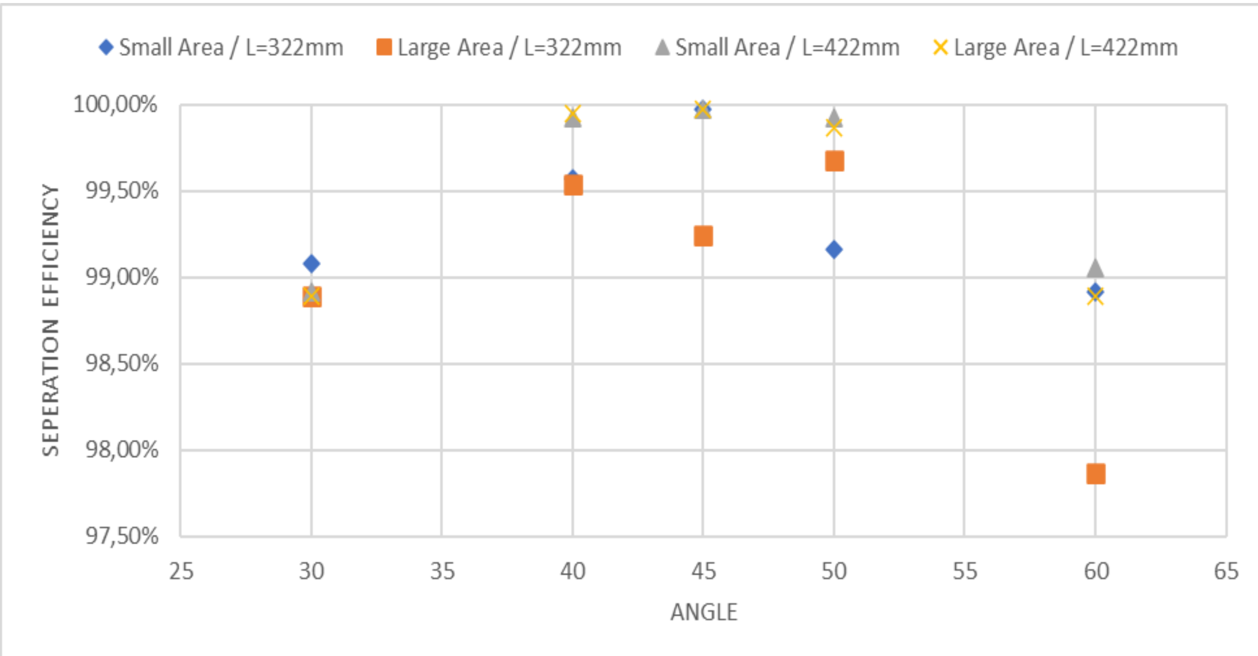

Figure 5: Condense Seperator Dimensions vs Separation Efficiency (%)

When this graph is examined in detail, it is seen that the parameter that most significantly affects the separation efficiency is the vane angle. When the angle is around 40-45-50, maximum separation efficiency can be obtained from the seperator. When the angle is at 30 and 60 degrees, the separator becomes inefficient, which is related to the throat velocity of the air in the vanes. When the effect of the throat area on the separation efficiency is examined, it is not correct to make a very accurate generalization. In some cases, efficiency is higher when the area is larger, and in some cases, efficiency is higher when the area is small. Although the cyclone length is not as effective as the angles, it can be seen that extending the cyclone length increases the separation efficiency. Since our criterion for separation efficiency is minimum 99.8% efficiency, 40,45 or 50 degrees will be chosen as an angle, for cyclone length 422 mm is chosen.

For the continuation of the optimization, the pressure drops at these 20 points were examined. Since the energy efficiency in the compressors is very important, even the savings in the condensate separator will provide savings to the end users.

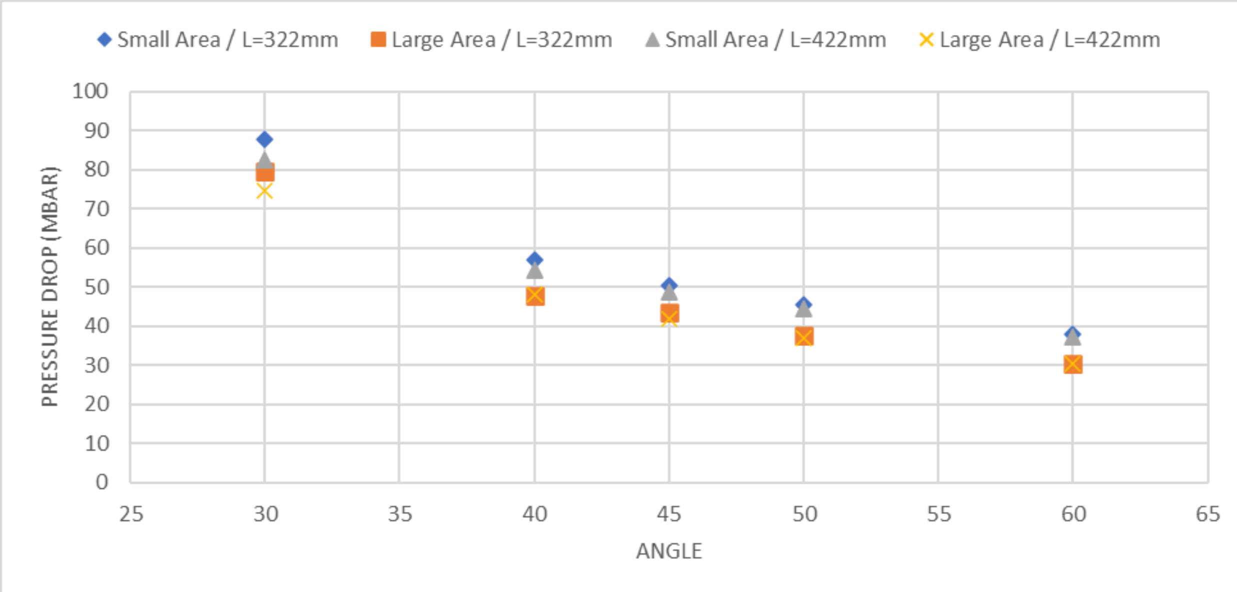

Figure 6: Condense Separator Dimensions vs Pressure Drop (pa)

When the graph is examined, the effect of the angle on the pressure drop is seen very clearly, as the angle increases, the pressure drop decreases. The reason for this is due to the enlargement of the area and the decrease in the average flow velocity values.

In the previous comparison chart, an angle of 40, 45 or 50 degrees was required to achieve the desired separation efficiency. For the cyclone length 422 mm was chosen for higher efficiency. Between these angles, the lowest pressure drop is reached at 50 degrees. As for the throat area, it is appropriate to choose the one with a larger throat area. It provides a reduction in energy consumption of 0.9 kW for every 10 mbar improved in pressure drop in a 110 kW compressor. Considering important issues such as pressure drop and separation efficiency, 99.86% efficiency is obtained as a result of CFD with the selected geometric dimensions.

4.2 Test Results and Validation

After 20 CFD studies were carried out, the design of the condensate separator was made with these selected geometric parameters, and the validation of the produced condensate separator was made with tests.

Table 2 CFD vs Test Result Comparison Table

Condition and Results	CFD	TEST
Ambient Pressure (barg)	1	0,997
Outlet Pressure (barg)	8	8
Compressor Inlet Temp.	20	20
Air cooler Outlet Temp	30	30
Relative Humidity (%)	80%	58%
Mass Flow Inlet (kg/s)	0,03727	0,002316
Trapped Mass Flow (kg/s)	0,03722	0,002306
Separation Efficiency (%)	99,86%	99,60%
Pressure Drop (mbar)	37	38,2

In the CFD reference conditions, the values in the table above are indicated, especially by specifying the high relative humidity, the situation in more difficult conditions can be seen. test conditions were very close to CFD conditions except for relative humidity. The amount of water expected to enter the condensate separator was calculated by measuring compressor operating pressure, ambient pressure, relative humidity, flow rate, compressor inlet and cooler outlet temperatures. Considering the amount of condense drained at the outlet of the condense separator, 99.6% of the theoretically expected amount of water has been drained. These test results and the values obtained in the CFD results have been confirmed, the reason for only 0.26% difference is because there are many parameters and the measurement tolerances of the measuring devices.

There is a tolerance of approximately 3.1% between the results of CFD and test for pressure drops, which is due to the effect of both production tolerances and ambient conditions. It is an acceptable ratio in the condensate separator for pressure drop deviation.

5. CONCLUSIONS

In this study, condensate separator design, CFD optimization and test validation of double-stage oil-injected, energy-efficient 90-110 kW power group screw compressors were performed. Before this study was carried out, the condense separator used in these compressors was purchased from the supplier. As a result of this study, with the designed efficient condensate separator, the separator dimensions were optimized, the separation efficiency was maximized and the pressure losses were optimized. Since we had dimensional problems in machine design, we designed an integrated water separator inside the compressor. While doing this, the most optimum design with high separation efficiency and low pressure losses that can be achieved in these dimensions has emerged as a result of 20 CFD optimization. At the compressor outlet, there will be almost no condensate in the compressed air going to the customer, plus it will contribute to energy efficiency with low pressure loss.

NOMENCLATURE

D_{iv}	Vane Internal Diameter (mm)
N_v	Number of Vane Elements
D_{ov}	Vane Outer Diameter (mm)
t	Swirl Vane Thickness (mm)
Re	Reynolds Number
We	Weber Number
V_{th}	Throat Velocity (m/s)

REFERENCES

Hoffmann, A. C., & Stein, L. E. (2010). Gas Cyclones and Swirl Tubes: Principles, Design, and Operation (Softcover reprint of hardcover 2nd ed. 2008 ed.). Springer.

Boles, M.A., Çengel Y.A., (2006). Thermodynamics and Engineering Approach, Fifth Edition, Mc Graw-Hill Book Co., New York.

Hanlon, P.C., (2001). Compressor Handbook, Mc Graw-Hill Book Co., New York.

Feng, J., Chang, Y., Peng, X., & Qu, Z. (2008). Investigation of the oil—gas separation in a horizontal separator for oil-injected compressor units. Proceedings of the Institution of Mechanical Engineers, Part A: Journal of Power and Energy, 222(4), 403–412. https://doi.org/10.1243/09576509jpe550

Yuan NG, S. (2005, January). Gas-Liquid Separation Using Axial Flow Cyclones. University Of Sheffield.

Peng, W., Hoffmann, A., Dries, H., Regelink, M., & Stein, L. (2005). Experimental study of the vortex end in centrifugal separators: The nature of the vortex end. Chemical Engineering Science, 60(24), 6919–6928. https://doi.org/10.1016/j.ces.2005.06.009

ACKNOWLEDGEMENT

We would like to thank Dalgakıran Compressor for encouraging the publication of our work.